Progressive Damage of Unidirectional Graphite/Epoxy Composites Containing a Circular Hole

FAN YANG AND C. L. CHOW*
Department of Mechanical Engineering
University of Michigan-Dearborn
Dearborn, MI 48128-1491

(Received April 23, 1996)
(Revised May 7, 1997)

ABSTRACT: In this paper, experimental and finite element results are presented to describe the anisotropic states of stress, strain and damage of unidirectional graphite/epoxy composite plates containing a central hole subjected to off-axis uniaxial tension. The nonlinear stress analysis of the laminates is based on the finite element procedure formulated with a newly developed anisotropic damage model, in which the inelastic behavior of composite material is attributed to the irreversible thermodynamics processes involving energy dissipation and stiffness change primarily caused by the presence of micro-structural changes of the material. Moiré interferometry, a high sensitivity whole-field experimental technique, with a computer image processing system is used to determine and to interrogate the two-dimensional deformation field in the composites. Results from the tests and analysis clearly reveal the anisotropic damage characteristics and the influence of principal material direction on the deformation response of the composites. Failure of the composite material near the hole area takes the form of a damage zone and the damage mechanism involves redistribution of stress and strain. From the analysis, it may be concluded that macrocrack initiates at the material point near the hole boundary with high damage value and propagates along the direction of damage zone extension. Good agreement between the predicted and experimental results confirms that the current approach can provide a convenient and accurate means to interrogate the complicated damage behavior of notched unidirectional composites with a hole and can be readily extended to examine the damage response of unidirectional composite structures with different notch configurations.

INTRODUCTION

FIBER-REINFORCED COMPOSITE LAMINATES continue to replace conventional metals in secondary and primary engineering structures owing to their high strength-to-weight and stiffness-to-weight ratios. Their mechanical response and

*Author to whom correspondence should be addressed.

0021-9983/98/06 0504–22 $10.00/0

failure behavior, therefore, have attracted considerable research interest in the last several decades. Past investigations [1] have revealed that these materials exhibit extremely complex damage modes under different loading conditions. The failure of composite laminates is accompanied by one or more of the following phenomena: fiber splitting, delaminations around free edges or at stress concentrations, matrix crazing, and transverse cracking of the plies with fibers oriented in a direction inclined to the loading directions. These phenomena must be taken into consideration in the evaluation of composite durability and structural reliability. To characterize these defects and their evolution involves techniques and methods for determining combined stress states in composite laminates and the subsequent application of failure criteria.

The methods to develop and refine models and procedures for determining progressive composite failure including the characterization of damage propagation and failure mechanisms in laminates may be based on either micromechanics or macromechanics. Micromechanics theories are usually proposed to model microcrack growth in an originally linear elastic brittle solid. In the cases of nonlinear material behavior, coupled with distributed interacting microcracks, derivation of microcrack kinetic laws presents a tremendous challenge. As the nucleation and the growth of distributed microscopic cavities and cracks will not only induce the occurrence of macro-cracks, but also lead to the deterioration of the material properties, i.e., reductions in strength, stiffness and fracture toughness, macromechanics conventionally calls this phenomenon of progressive degradation of the material prior to its final fracture as damage. Because the complexity of material damage in fiber reinforced composite laminates renders an exact analytical solution describing the fine details of a particular damage type untenable, it is rational to consider the locally averaged effect of the damage as overall response of the material. Based on the thermodynamics of irreversible process, a set of internal state variables is used to model the material damage state and its evolution equation to describe the response of material with progressive damage. This approach is usually referred to as Damage Mechanics.

Recently, Allix et al. [2], Kamimura [3], Talreja [4], and Allen and Lee [5] presented some damage models for composite laminates. In their models, damage entities are represented by an appropriate set of vector- or tensor-valued internal state variables with which the constitutive relations for elastic composite with distributed damage are formulated. Although these investigations offer a way to incorporate the micromechanics level damage mechanisms into macromechanics failure models, their attentions are focused at the prediction of stiffness loss of a laminate for a given damage state, while the stress-strain responses of the laminate with damage are not fully addressed. The phenomenological approach developed in Reference [6], however, differs from these mechanics models in that it has the advantage in describing the evolution of the stress states in a composite as material damage progresses due to mechanical loading.

The behavior of fiber reinforced composite laminates with stress concentrations such as cutouts is of practical interest in the design analysis of composite structures because of the resulting significant variations of strength reduction and the damage growth around these stress concentrations in service. In order to employ

composites in practice with confidence, it is necessary to evaluate their tolerance to flaws and stress concentrations. A great deal of experimental and analytical work has been conducted to evaluate the behavior of composite laminates with holes. While the importance of the problem has been well recognized, understanding of the fundamental nature of the problem is still very limited due to its inherent complexities.

Stress and strain distributions in composite plates around stress concentration, such as holes or cracks, have been treated analytically using linear anisotropic elasticity and finite element methods. The latter one can be used to account for material inhomogeneity, nonlinearity and inelasticity. Some experimental methods such as strain gages, photoelastic coatings and moiré technique have proven very useful in verifying theoretical solutions in the linear range and extending them in the nonlinear range. Experimental approaches are especially useful in studying failure modes and analyzing the effects of damage in composites.

This paper is concerned with the prediction and examination of the behaviors of the unidirectional graphite fiber reinforced composites containing a circular hole. The behaviors of unidirectional lamina should be better understood before an attempt is made to examine laminate behaviors. The latter one problem is inherently more complex since generally a three-dimensional stress state exists in a multilayer laminate containing a hole. The anisotropic damage model proposed in Reference [6] and the finite element procedure developed in Reference [7] are employed to study the problem. An experimental technique, moiré interferometry, is introduced to observe the behaviors of the notched unidirectional composite laminates under off-axis tensile loading. Validation of the proposed anisotropic damage model is achieved by comparing the predicted results with the experimental ones.

CONSTITUTIVE RELATION FOR COMPOSITE LAMINA WITH DAMAGE

As the current attention focuses on the inelastic behavior of composite lamina with damage, the method introduced in Reference [6] is employed here. The deviation of the elastic response of the composite ply is considered as a result of the nucleation of new damage entities and the growth of existing damage entities. This problem can be solved by constructing a damage surface in stress space, which also represents initial and subsequent damage surface in stress space. The elastic region is defined as the loci of stress paths along which the damage does not change. This damage surface may be expressed by

$$F(\sigma_i, D) = 0 \tag{1}$$

It is a function of the state of stress σ_i ($i = 1,2,...,6$, here, the contracted notation is utilized) and the internal variable D. D is a measure of damaged deformation and hence changes only when damage progresses. F is assumed to be continuously differentiable with respect to its arguments. When the stress state is within F, the behavior of the material is elastic; if the stress point reaches the boundary F, i.e., if F

= 0, a subsequent increment of stress may either cause purely elastic deformation or lead to damage process depending on the direction of the increment. Therefore, similar to the flow rule in the plasticity theory, the incremental damaged strain may be evaluated based on the damage function F,

$$d\varepsilon_i^d = \begin{cases} d\lambda \dfrac{\partial F}{\partial \sigma_i} d\lambda > 0, & \text{when } F = 0 \text{ and } \dfrac{\partial F}{\partial \sigma_i} d\sigma_i > 0 \\ 0, & \text{otherwise} \end{cases} \tag{2}$$

where the superscript d refers to the damaged strain component, and $d\lambda$ is a scalar of proportionality and can be determined from the consistency condition $dF = 0$. This consistency condition implies that the stress state σ_i always lies on the boundary of surface F during a process of damage.

Here, the energy dissipation per unit volume is selected as damage variable and its increment can be written as

$$dD = \frac{1}{2}\sigma_i d\varepsilon_i^d \tag{3}$$

The summation convention is employed wherein a repeated index implies summation over its range.

If time, rate, and environmental effects such as temperature and moisture are excluded and deformation is small, the total strain components ε_i of composite lamina in a fixed damage state can be expressed through the following stress and strain relation

$$\varepsilon_i = C_{ij}\sigma_j \quad \text{or} \quad \sigma_i = S_{ij}\varepsilon_j \qquad \text{(for fixed } D\text{)} \tag{4}$$

in which C_{ij} ($C_{ij} = C_{ji}$) and S_{ij} ($S_{ij} = S_{ji}$) are the current material elastic compliance and stiffness, respectively, and $[S_{ij}]^{-1} = [C_{ij}]$, if the inverse exists.

In a damage process, from Equation (4), the total strain increment can be linearly decomposed into elastic and damaged portions:

$$d\varepsilon_i = C_{ij}d\sigma_j + dC_{ij}\sigma_j = d\varepsilon_i^e + d\varepsilon_i^d \tag{5}$$

where the superscript e stands for the elastic strain component. Thus, one has

$$d\varepsilon_i^e = C_{ij}d\sigma_j \quad \text{and} \quad d\varepsilon_i^d = dC_{ij}\sigma_j \tag{6}$$

From Equations (5) and (6), one has

$$d\sigma_i = S_{ij}(d\varepsilon_j - d\varepsilon_j^d) \tag{7}$$

and after determining the damaged strain increment from Equations (1), (2) and (3) as well as the consistency condition, the relationship between the elastic-damaged stress increments and the total strain increments can be finally expressed as

$$d\sigma_i = S_{ij}^{ed} d\varepsilon_j \tag{8}$$

where

$$S_{ij}^{ed} = S_{ij} - \frac{S_{ik}\dfrac{\partial F}{\partial \sigma_k}\dfrac{\partial F}{\partial \sigma_1} S_{lj}}{\dfrac{\partial F}{\partial \sigma_m} S_{mn} \dfrac{\partial F}{\partial \sigma_n} - \dfrac{1}{2}\dfrac{\partial F}{\partial D}\sigma_p \dfrac{\partial F}{\partial \sigma_p}} \tag{9}$$

is the elastic-damaged instantaneous tangent modulus matrix. It should be noticed that the values of S_{ij} in this equation are not constants anymore. Usually, S_{ij} is a function of stress state and is dependent upon the previous loading histories that involve damage progression.

With the postulation that damage effects are reflected through the variation of material elasticity and the material coefficients C_{ij} are merely a function of damage state D, independent of the damage process [8], the compliance of the material element at any damage state can be expressed as

$$C_{ij}(D) = C_{ij}(0) + \int_0^D \frac{2}{P}\left(\frac{\partial^2 F}{\partial \sigma_i \partial \sigma_j} + \frac{1}{P}\frac{\partial F}{\partial \sigma_i}\frac{\partial F}{\partial \sigma_j} - \frac{1}{P}\frac{\partial F}{\partial \sigma_i}\frac{\partial^2 F}{\partial \sigma_j \partial \sigma_u}\sigma_u - \frac{1}{P}\frac{\partial F}{\partial \sigma_j}\frac{\partial^2 F}{\partial \sigma_i \partial \sigma_m}\sigma_m + \frac{1}{P^2}\frac{\partial F}{\partial \sigma_i}\frac{\partial F}{\partial \sigma_j}\frac{\partial^2 F}{\partial \sigma_r \partial \sigma_p}\sigma_r \sigma_p\right) dD \tag{10}$$

where $C_{ij}(0)$ denotes the compliance components of the material without damage and $P = (\partial F/\partial \sigma_u)\,\sigma_u$. Equations (4), (8), (9), and (10) formulate a general constitutive description for an elastic-damaged composite material element.

As an example, consider a damage surface represented as

$$F(\sigma_i, D) = (R_{mn}\sigma_m \sigma_n)^{1/2} - K(D) = 0 \tag{11}$$

where the coefficients R_{ij} ($R_{ij} = R_{ji}$ is assumed) depict the influence of each stress component on the material damage state and can be determined from experiments, and $K(D)$ is a state function which changes as D develops. Furthermore, the equivalent stress σ_o and the equivalent damaged strain increment $d\varepsilon^d$ are defined as

$$\sigma_o^2 = R_{mn}\sigma_m \sigma_n \quad \text{and} \quad 2dD = \sigma_i d\varepsilon_i^d = \sigma_o d\varepsilon^d \tag{12}$$

and $\sigma_o - \varepsilon^d$ relation established from experiment is

$$\varepsilon^d = m\sigma_o^n - m\sigma_s^n \tag{13}$$

where m and n are positive constants, σ_s is the equivalent stress at the threshold of damage. From Equations (10) and (12), the following equations can be derived,

$$C_{ij}(D) = C_{ij}(0) + \frac{mn}{(n-1)}(\sigma_o^{n-1} - \sigma_s^{n-1})R_{ij} \tag{14}$$

and

$$D = \frac{mn}{2(n+1)}(\sigma_o^{n+1} - \sigma_s^{n+1}) \quad (\text{for } d\sigma_o \geq 0) \tag{15}$$

From Equation (14), it can be seen that the coefficients R_{ij} reflect the anisotropic behavior induced by material damage. During a damage process, Equation (14) is employed to predict instantaneous C_{ij} values. For unloading, the coefficients C_{ij} remain constant and are determined from σ_o at the start of unloading. Upon reloading, D and C_{ij}, do not change unless σ_o exceeds its previous maximum value. Schapery [8] has proven that for unloading, $d\sigma_o < 0$, the thermodynamic requirement of positive entropy production and the path-independence of the unloading work are violated unless D is constant. Consequently, for arbitrary stress histories, D is always determined by the largest value of σ_o up to the current time.

To provide a validation analysis of the proposed damage theory, a comparison between experimental measurement and theoretical prediction of response of composite laminates is performed in the following sections.

THEORETICAL CONSIDERATIONS

To provide rigorous solutions to the general response of notched composite laminates with damage, numerical integration algorithms for the general incremental load-deformation analysis of composite laminates based on the proposed lamina model have been systematically explored in Reference [7] with the context of displacement-based finite element method. The displacements of the finite element assemblage are assumed to be infinitesimally small so that only material nonlinearity due to damage needs to be included. The procedure for implementing the corresponding finite element equations is similar to the conventional nonlinear analysis. The main difference lies in the stress-strain relations, which currently include a damage variable. Therefore, the modification of the stiffness matrix during the calculation of progressive damage process is necessary.

The problem under investigation is illustrated in Figure 1, where a unidirectional, rectangular, fiber reinforced composite plate of dimensions L, W with a circular hole radius R is subjected to far-field uniaxial tensile stress p. Under such cir-

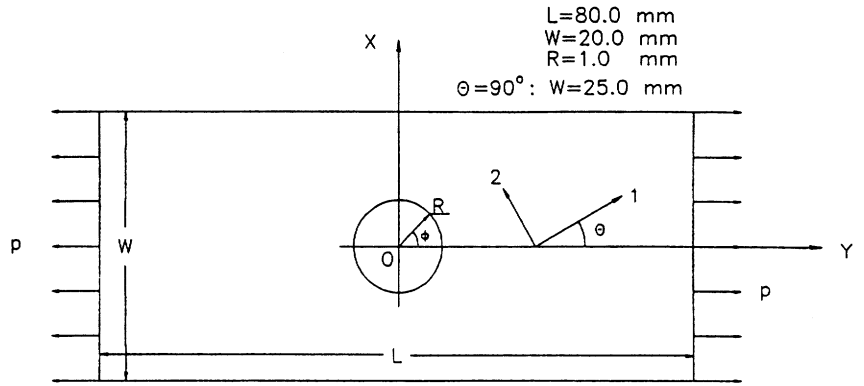

Figure 1. *Unidirectional laminate with a hole subjected to tension.*

cumstances, the composite laminate is in a state of plane stress and only three stress components σ_{xx}, σ_{yy} and σ_{xy} need to be considered. Two coordinate systems, global coordinates x-y and material principal system 1-2 are set at the center of the hole. θ stands for the fiber orientation angle between the loading direction and the maximum principal material axis. Boundary conditions are such that the ends ($y = \pm L/2$) remain plane and parallel. This is intended to simulate perfect gripping and no rotation of the grips. The corresponding material coefficients of the composite lamina presented in Reference [6] will be used as input data.

Theoretical solutions for the problem are obtained with an incremental scheme using the developed two-dimensional finite element program. Because of the non-symmetrical nature of the specimen, the whole off-axis unidirectional composite laminate is modeled with 96 plane-eight-node isoparametric elements consisting of 328 nodes and the finite element mesh is refined near the hole area as shown in Figure 2. The numerical solution allows damage to initiate and to accu-

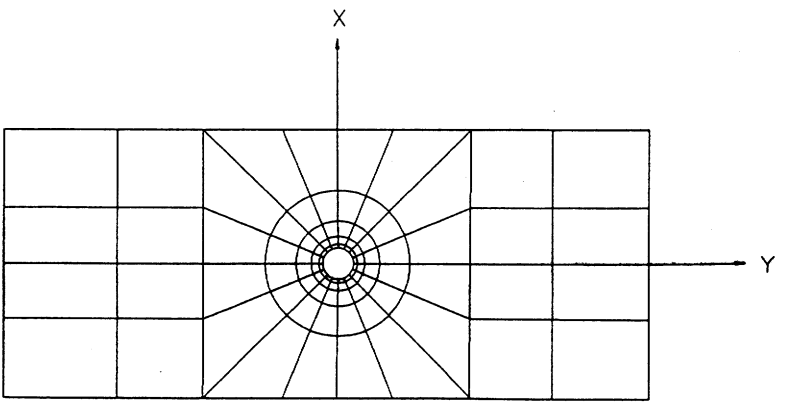

Figure 2. *Finite element modelling for the lamina with a hole.*

mulate throughout the specimen as a field quantity, and the changes of the stiffness due to the coupling between damage and elasticity. The linear elastic analysis for the laminate without damage consideration is first conducted to identify the stress and strain concentration points possible for damage emergence. The loading of the notched composite specimen is then applied incrementally to observe the initiation and propagation of damage zone.

EXPERIMENTS

Moiré interferometry [9], with its potential for revealing displacement fields with high sensitivity for analysis of damage in composites [10], has been applied to study the deformation in the specimen. This technique is typically practiced by replicating a high-frequency specimen grating on the surface of the specimen. The grating will deform together with the underlying specimen. A reference grating, usually a virtual grating formed by the intersection of two coherent beams, is superimposed on the specimen grating. The result is a moiré pattern formed by interaction of the specimen grating and reference grating. From optical consideration, the frequency of the virtual reference grating is adjusted to twice that of the specimen grating. Then, when the specimen is loaded, the displacement u or v of every point is mapped by the moiré fringe pattern and interpreted by

$$u = \frac{1}{f} N_x \qquad v = \frac{1}{f} N_y \tag{16}$$

where N_x and N_y are fringe orders at the corresponding point along the x- and y-axis, respectively, and f is the frequency of the reference grating which is 2400 lines/mm here.

For this investigation, a moiré interferometry device shown in Figure 3 was designed and constructed so as to allow measurement of both components of in-plane displacement field on the specimen surface [11]. A 135 mW He-Ne laser LB provides a monochromatic and coherent light. The laser beam is reflected by mirrors M1 and M2 into a spatial filter SF. The spatial filter contains a microscope objective which focuses the laser light at a point and diverges it beyond that point. A pinhole is positioned at the focal point in order to strip off light originating from the nonuniform exterior of the laser beam. The diverging beam of light is reflected by a parabolic mirror PM, the collimating element, to the specimen and mirrors MA, MC and MB. The light coming from the collimator is a beam of collimated, coherent, and monochromatic light. The light illuminates the mirror surface MB and the specimen to obtain the transverse moiré pattern. The two 45 degree mirrors MA and MC are adjusted to direct portions of the collimated beam at angles $+\alpha$ and $-\alpha$ in the vertical plane, to form the longitudinal moiré pattern. The viewing light from the specimen S encounters a beam splitter BS which divides the beam into two essentially equal parts. One part of the beam passes through the BS and the camera lens CL to a video camera VC which is utilized to monitor the localized hole area of the specimen. Another part of light emerging from the BS, the beam

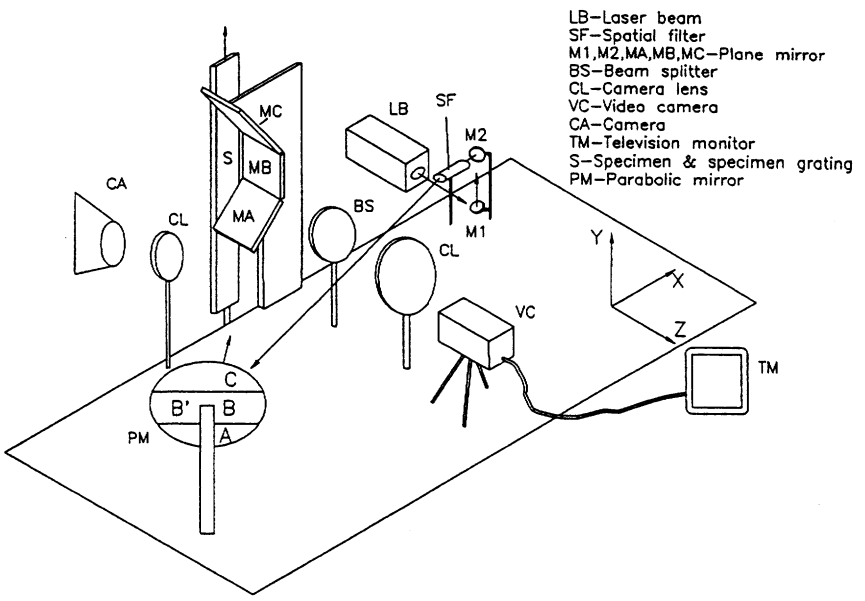

Figure 3. *Optical arrangement for moiré interferometry.*

reflected by the BS, goes to a photographic camera CA which is employed to observe the global response of the specimen. These cameras are used to capture the moiré fringe patterns for subsequent image processing. As the arrangement presented is quite sensitive, all of the optical elements and the specially designed displacement screw-loading frame connected with a load cell are firmly mounted on a stiff and massive metal table.

When employing the apparatus described above, the two in-plane displacement fields are examined independently. To obtain the N_y or v field on the camera screens, a sheet of opaque cardboard is inserted in front of the parabolic mirror (PM) to block portions B and B' of the incident collimated beam of light that provides the transverse moiré pattern. The N_x or u field appears when the card is placed on the PM such that portions A and C are blocked. The actual procedure for the moiré interferometry test is relatively straightforward: (1) install the specimen in the loading fixture; (2) adjust the mirrors MA, MC, and MB for initial displacement u and v fields and capture them as reference states; (3) apply loads to the specimen and photograph the u and v fields.

Generally, when there is no load applied to the specimen during the test, an initial fringe pattern is observed due to the high sensitivity of the moiré interferometric method along with imperfect optics. In most cases, the "null-field" pattern is sparse and can be ignored. However, if necessary, it can also be subtracted from the final pattern to yield the moiré fringes showing displacement contours due to the applied load exclusively. Sometimes, by changing the angle "α" of the two incident light beams, a carrier or bias fringe pattern is formed, which can be used to

provide monotonically varying fringes, and superposed on the moiré pattern under a particular load. This technique is quite useful in assisting subsequent computer image processing.

RESULTS AND DISCUSSIONS

The extent of damage from the edge of a central hole in unidirectional composite laminates will be examined in detail in this study. The unidirectional graphite/epoxy systems with fibers oriented along $\theta = 0°, 22.5°, 45°, 67.5°$ and $90°$ are considered. The measured properties of initial undamaged lamina made of 648 epoxy matrix reinforced by 65 volume percent of T300 graphite fibers are [6]

$$E_{11} = 1.25 \times 10^5 \text{ MPa}, \qquad E_{22} = 1.11 \times 10^4 \text{ MPa},$$

$$\nu_{12} = 0.338, \qquad E_{66} = 3.3 \times 10^3 \text{ MPa}$$

Experimental information on $\varepsilon_x - \sigma_x$ behavior for two fiber angles has been used to evaluate R_{66} and the function $\varepsilon^d(\sigma_o)$. The corresponding material coefficients in Equations (11) and (13) are

$$m = 0.114 \times 10^{-4}, \qquad n = 1.242, \qquad \sigma_s = 9.0 \text{ MPa}$$

$$R_{11} = R_{12} = R_{16} = R_{26} = 0, \qquad R_{22} = 1.0, \qquad \text{and } R_{66} = 1.9$$

Results from tests at other fiber angles then serve to check the formulation.

Shown in Figure 4 are the damage contours of the composite specimen with zero degree fiber orientation. Damage is first observed at the point of $\phi = 64.9°$ (and

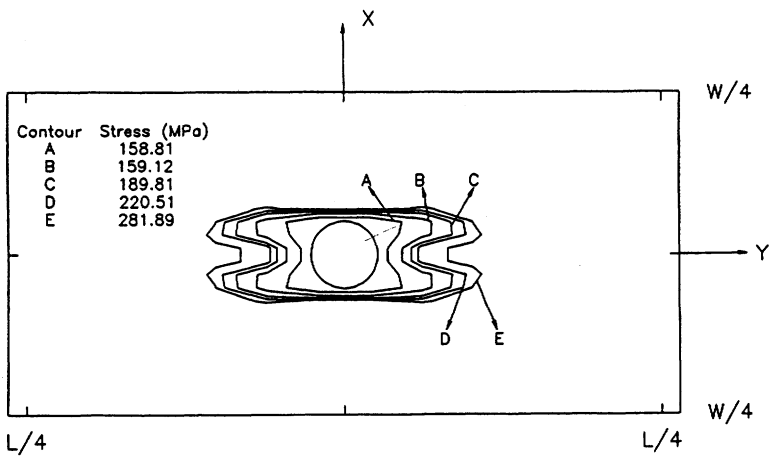

Figure 4. *Damage contours for laminate with $\theta = 0°$.*

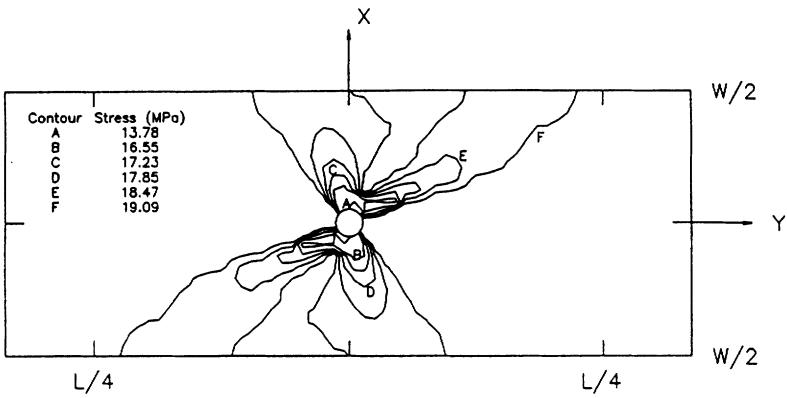

Figure 5. *Damage contours for laminate with $\theta = 22.5°$.*

–64.9° due to the symmetry of the laminate) on the hole edge when the applied stress p is 35.95 MPa. Theoretical analysis indicates that the combination of normal and shear stress components at that point leads to a higher equivalent damage stress than those of other points. Damage value of this point increases with the increase in applied load causing the formation of damage zone and extending not perpendicular to but along the loading direction which is the weakest region in the composite. From this damage zone pattern, it may be expected that crack will initiate at the point of maximum damage magnitude and the angle of crack propagation will be along the applied loading direction.

For the 22.5° specimen, the material point on the hole edge at $\phi = 70.07°$ (and 250.07°) first experienced damage as the applied stress reached the level of 8.14 MPa. The damage zone contours of the specimen are depicted in Figure 5. It can be observed from the figure that the damage zone expands from the hole boundary towards the specimen edge along the composite material principal directions during the loading process. The damage values of the material element in the fiber direction are higher than those perpendicular to the fibers. This implies that failure of the specimen initiating from the hole edge will be along the fiber direction, i.e., $\phi = 22.5°$.

The damage zones of 45° and 67.5° specimens are presented in Figure 6 and Figure 7 respectively. The external stress level to trigger the damage in the material is 4.91 MPa for 45° specimen, and 3.79 MPa for 67.5° laminate. The damage initiation position is on the hole edge at $\phi = 78.75°$ (and 258.75°) for both cases. Similarly, development of the damage zones in these laminates is also along the material principal directions.

The material point of 90° laminate on the hole edge at $\phi = 90°$ (and 180°) is found to suffer damage at the stress level of 3.62 MPa. Tension stresses near the hole boundary are mainly responsible for the damage initiation. Because of the special loading condition and specimen configuration, symmetric evolution of damage zone along the fiber direction perpendicular to the applied load is predicted as displayed in Figure 8. It is evident that the failure of the specimen will be

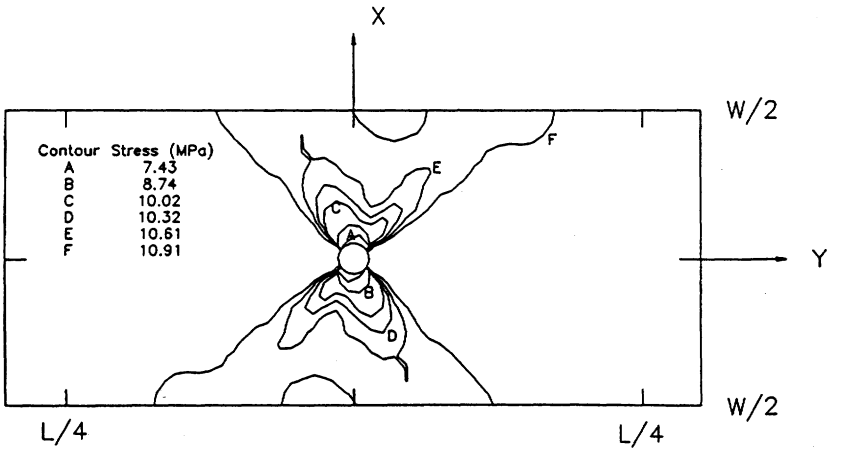

Figure 6. *Damage contours for laminate with $\theta = 45°$.*

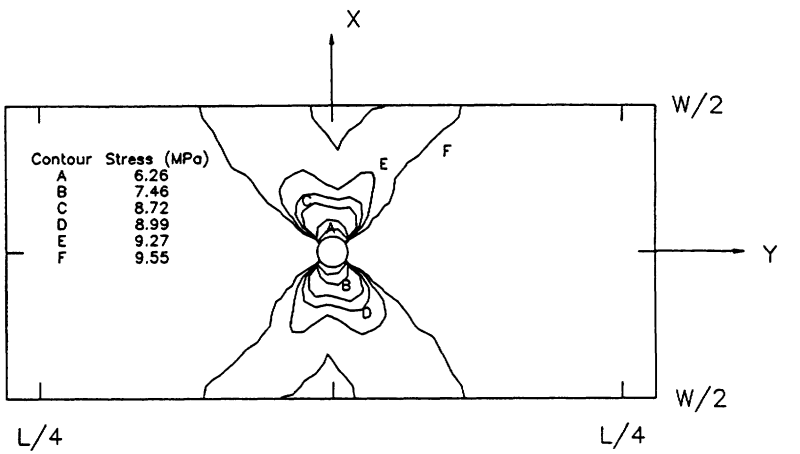

Figure 7. *Damage contours for laminate with $\theta = 67.5°$.*

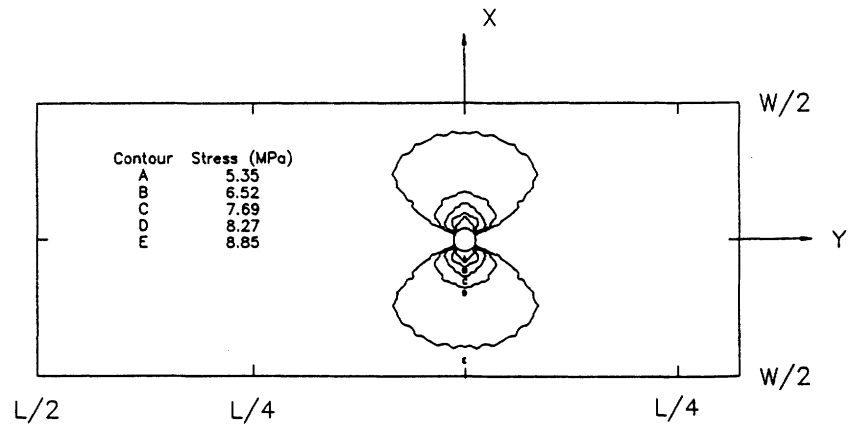

Figure 8. *Damage contours for laminate with $\theta = 90°$.*

along $\phi = 90°$ (and 180°) since damage of the material elements lying in that direction continues to accumulate and extend with increasing load application.

For the circular cutout under consideration, Figure 9 shows the relation between the calculated damage initiation stresses and fiber orientation of the unidirectional composite laminate. It can be seen from the curve that the level of stress causing damage initiation decreases as the angle θ between the direction of applied stress and fibers increases.

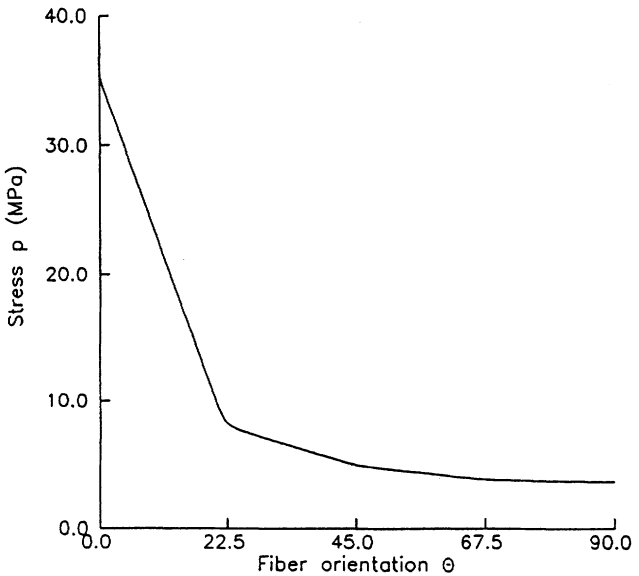

Figure 9. *The relation between damage initiation stress and fiber orientation.*

For illustrative purpose, the experimental results revealing deformation behavior of unidirectional graphite/epoxy laminates with fiber orientation angles $\theta = 0°$, 45° and 90° are presented here. Figure 10 shows the moiré patterns representing the contours of the displacement components along the x and y directions for the 0 degree specimen. The patterns (a) and (b) are the v-field and u-field fringes respectively when the far-field extension strain is about 1310 $\mu\varepsilon$. Also under this strain level, the patterns (c) and (d) corresponding to the displacement fringes in y and x directions respectively, are recorded by the video camera VC in Figure 3 zoomed in the vicinity of the hole area of the specimen. The pictures (e) and (f) display the whole-field v and u fringe patterns respectively, at an applied strain level 1780 $\mu\varepsilon$. The photographs shown in (a), (b), (e), and (f) are recorded by the photographic camera CA in Figure 3. It is seen that at higher applied load levels, both u and v patterns show significantly dense fringes near the hole area. This is attributed to very large strain value in the composite laminate specimen. In the patterns, a marked strain concentration area near the hole can be observed, a clear indication of the damage zone of the specimen. It is obvious that when the damage zone around the hole develops, it remains narrow, constrained to the immediate vicinity of the hole, and tends to propagate along the loading direction.

Presented in Figure 11 are the v and u patterns for the 45 degree specimen. In these pictures, (a) and (b) are respectively the whole-field v and u patterns for an applied load of 440 N, while (c) and (d) are respectively the v and u fringes under 1364 N. The close-up moiré fringes along y and x directions for an applied load of 1364 N are shown in (e) and (f) respectively. Generally, from these figures, it can be seen that as the load increases, there is an increase in strain concentration near the hole area; but the fringe pattern elsewhere is still uniform and smooth. At a higher load level, the fringe patterns in the figures become increasingly dense; however, the fringe contrast is still excellent, a credit to the moiré interferometric method. Also along the principal material direction of the specimens, i.e., 45° to the vertical x axis, a noticeable band where the fringe pattern, and hence the deformation, is different from the rest of the specimen, can be observed. These bands indicate increased damage of the composite as compared to other regions. The shapes of the patterns also elucidate greater shear as compared to the normal strain describing damage characteristics of unidirectional composite laminate.

Figure 12 displays the v and u deformation patterns for the 90 degree specimen. The load level for (a) and (b), the whole-field v- and u-displacement components respectively is 440 N. Pictures (c) and (d) are the whole-field fringe patterns corresponding to y and x directions for the load of 792 N respectively; while under the same load, photographs (e) and (f) are the localized v and u moiré fringes respectively. Similar to earlier cases, application of higher level loads leads to higher overall damage of the composite specimen. Bands of damage are also visible along the material principal direction, parallel to the vertical axis. Abrupt change in the moiré fringe pattern near the hole edge, which represents a macrocrack emergence, is evident as shown in pictures (c) and (e).

It should be pointed out that all the fringe patterns shown include their respective reference patterns which are some initial fringes, partly due to the imperfections in the optics and partly due to the small clamping load that has to be applied to

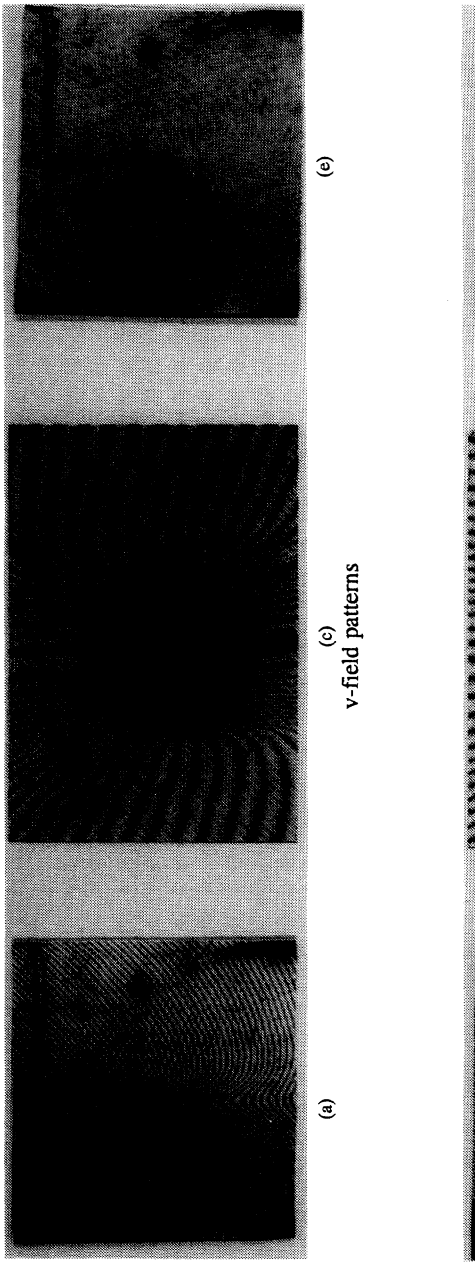

Figure 10. *Fringe patterns for 0° specimen.*

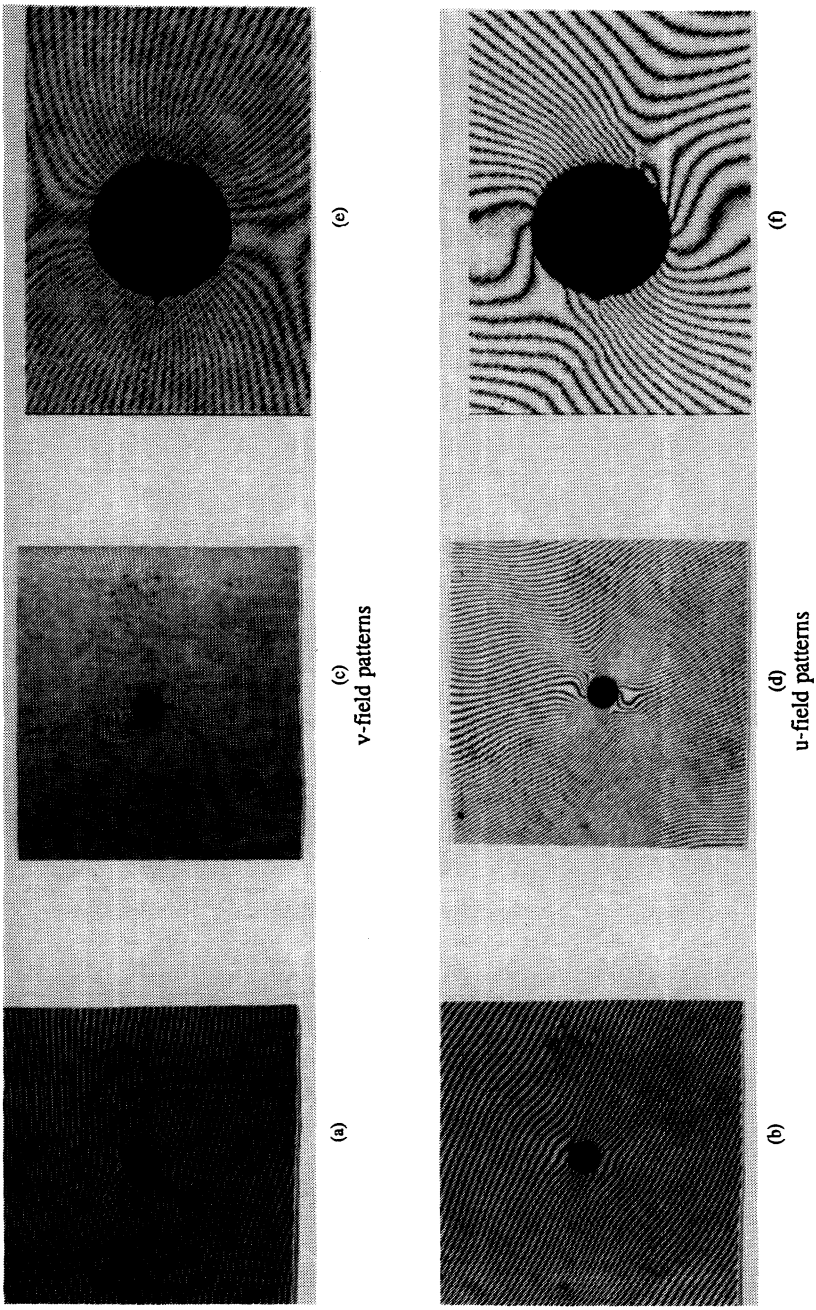

Figure 11. *Fringe patterns for 45° specimen.*

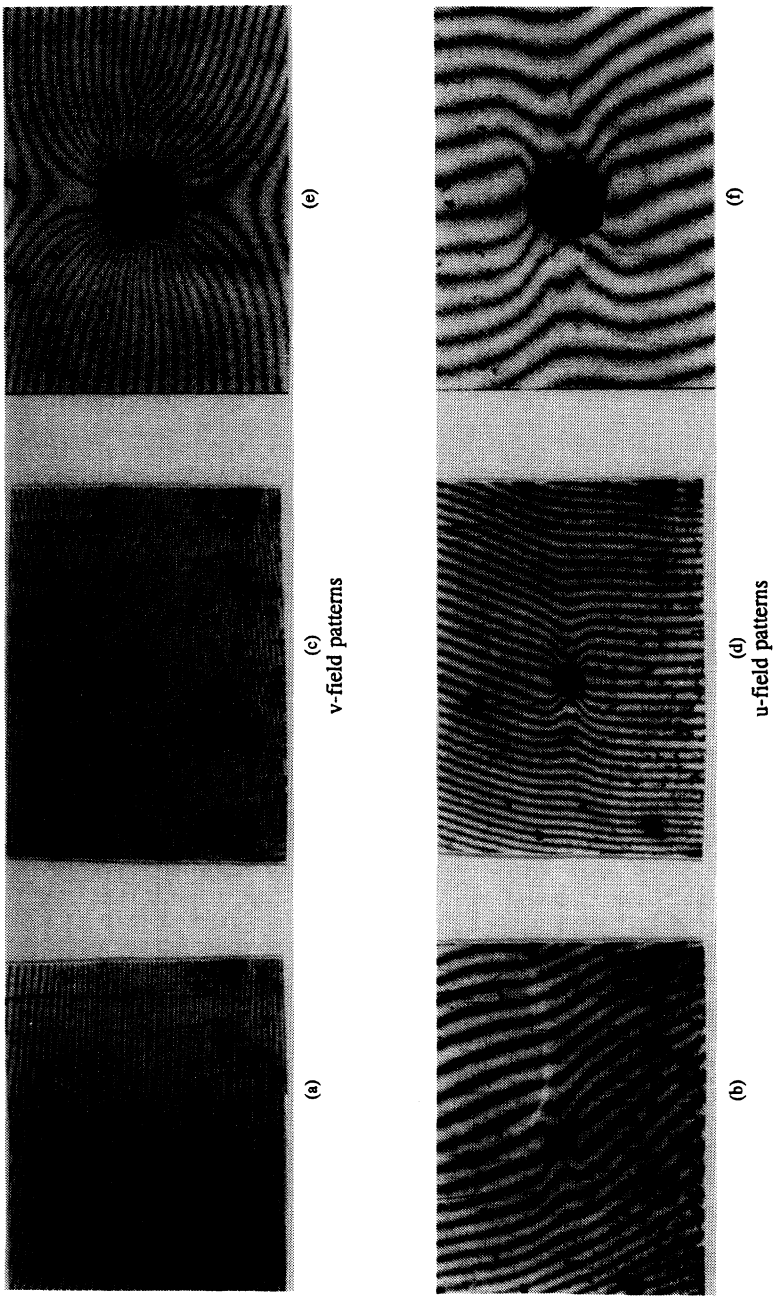

Figure 12. *Fringe patterns for 90° specimen.*

the specimen. This pattern should be subtracted from the subsequent patterns to obtain deformation information due to the external load alone. Furthermore, another usefulness of the carrier pattern is that it can be added initially to increase the density of fringes when the original pattern is sparse because of small deformation, or reduce the density of fringes as the original pattern is too dense due to large deformation of the specimen. This procedure is an important aid to the latter image processing in the calculation of displacement and strain of the specimen, which will be next discussed.

In order to check the validity and accuracy of the nonlinear behavior analysis for unidirectional composite laminate containing a circular hole with the proposed damage theory, a comparison between experimental measurements and theoretical predictions is performed. Quantitative evaluation of the moiré patterns taken from the experiment, even with computer processing, is very tedious and time consuming, considering that the pictures shown in Figures 10–12 are only a few samples of many pictures that were recorded at regular intervals. For simplicity, in what follows, one strain component ε_{yy} distribution along the vertical x axis is evaluated. Similar procedure can be applied to obtain other strain components. The developed image processing software to evaluate the displacement field of the specimen under a certain load level uses the fast Fourier transform (FFT) method, where the brightness function of a moiré image pattern is Fourier-transformed from which the frequency components of the image containing displacement information can be isolated [11]. Then, the strain distribution is given as derivative of the corresponding displacement with the aid of Equation (16).

In Figures 13 and 14, the prediction and measured results of the strain component ε_{yy} along the vertical x axis are compared for the 45° and 90° specimens under the loads 968 N and 440 N, respectively. Under the same external loading condition, the predictions from the conventional linear elastic theory with the original material stiffness without degradation, which are referred to as the pseudo elastic strains, are also included. It can be observed from the figures that the damage theory produces higher strain values and provides better prediction to the experiment strain distribution than that based on the linear elasticity theory. The discrepancy becomes more significant near the hole edge. The strain concentration effect is, as expected, enhanced due to damage existence. The difference in strain magnitude between the linear elasticity and nonlinear damage theory will become more pronounced with further damage development as the applied load increases.

Figures 15 and 16 show the distributions of the damage and the pseudo stress components σ_{yy} and σ_{xx}, and σ_{xy} of 45° and 90° specimens along the x-axis subjected to the overall load levels of 968 N and 440 N respectively. Here, the pseudo stresses are calculated from the pseudo elastic strains. Nonlinear influence due to damage on stress components σ_{yy} and σ_{xy} is much more pronounced than that on stress σ_{xx} in 45° specimen, while damage effect on stress σ_{yy} is more evident in 90° specimen. Here, it should be of interest to note that by disregarding the damage influence, the stress concentration at the edge of the hole under the current applied load level is overestimated for stress component σ_{yy}, as shown in Figure 15a and Figure 16. This will lead to the overestimation of overall strength of the unidirectional composites with a hole. The errors encountered in the global response analy-

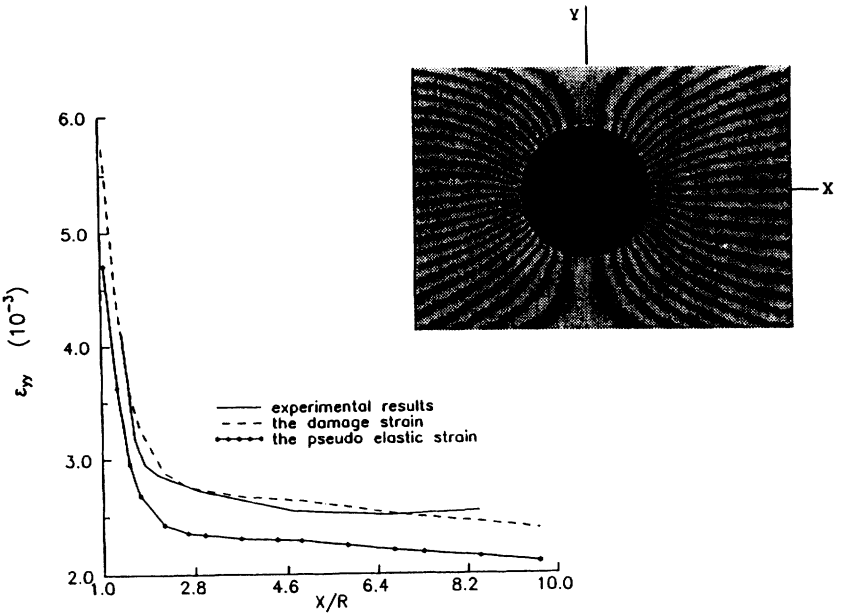

Figure 13. *Predicted and experimental strain ε_{yy} distribution along x-axis for 45° off-axis specimen.*

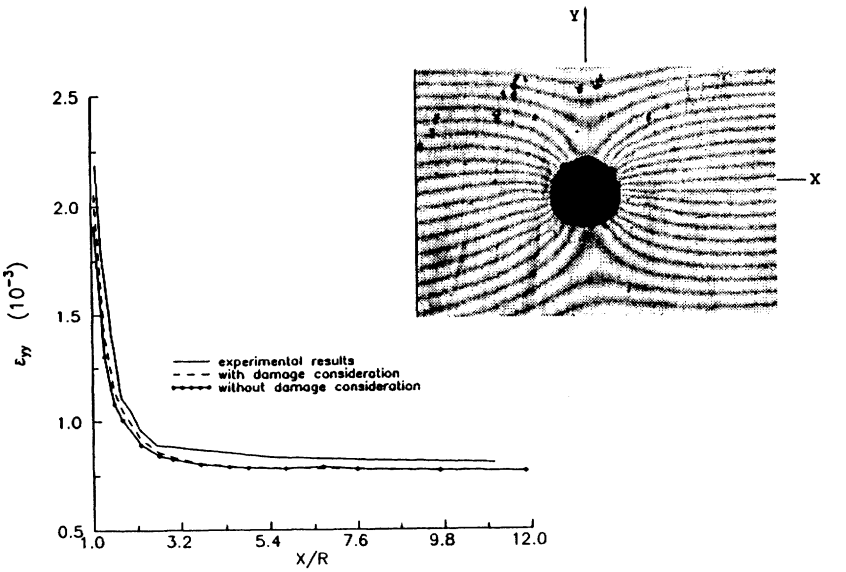

Figure 14. *Predicted and experimental strain ε_{yy} distribution along x-axis for 90° specimen.*

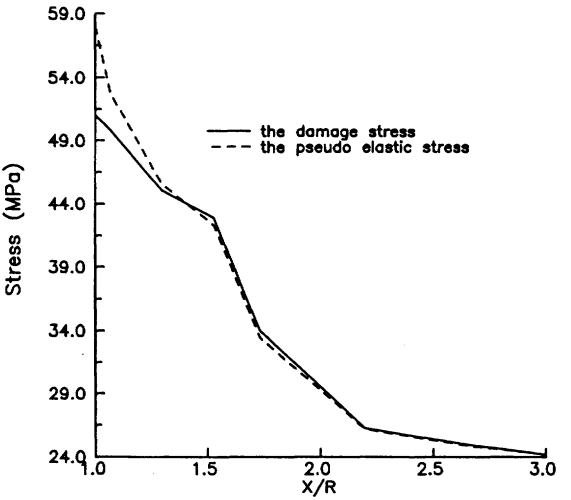

(a) σ_{yy} distribution

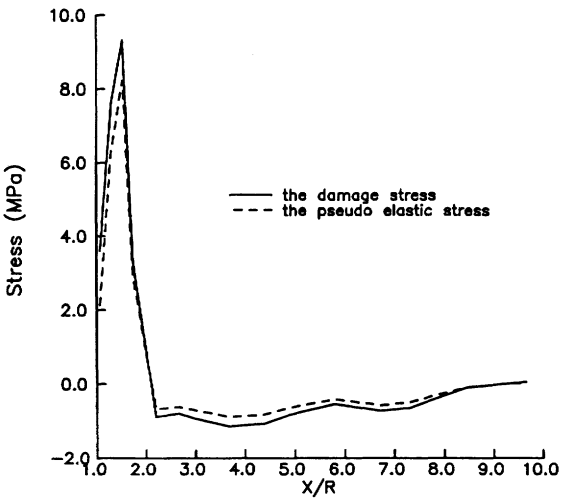

(b) σ_{xy} distribution

Figure 15. *Stress distribution along x-axis for 45° off-axis specimen.*

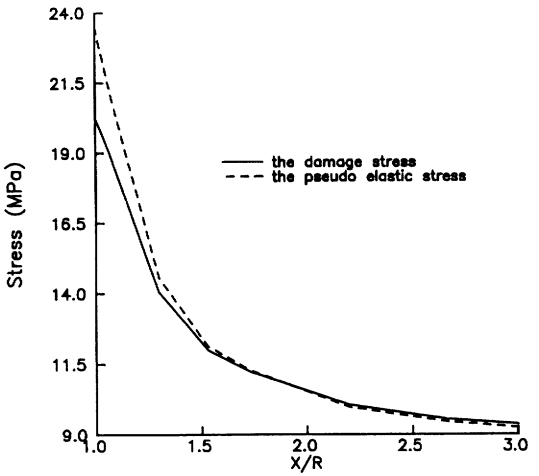

Figure 16. *σ_{yy} stress distribution along x-axis for 90° specimen.*

sis of the composites from linear elastic theory with the initial material stiffness without damage will be even larger when the applied load level is higher.

CONCLUSIONS

Both analytical and experimental techniques are very important tools required to advance the knowledge and understanding of progressive failure behaviors in composites. Analytically, in this paper, an anisotropic damage model has been employed to analyze the elastic-damaged nonlinear response of unidirectional composites containing a central circular hole. Damage is defined here as the material degradation at the "material element point" level. The prediction of in-plane response of a composite is achieved by using two-dimensional finite element analysis, from which the failure mode, damage zone and its development, has been identified. Results given from the numerical analyses conducted on unidirectional graphite fiber/epoxy composites under off-axis tension illustrate that the material coefficients of material elements in the damage zone will change, thus causing the redistributions of stresses and strains. These new stress distributions determine the subsequent development of damage zone and the load capacity of the composites. The strain distribution results from the predictions are in good agreement with those from the experiment.

Experimentally, on the other hand, moiré interferometry technique, due to its capability for displaying two-dimensional displacement fields for analysis of damage in composites, has been applied to study the deformation in the laminates with the aim of verifying the theoretical predictions. It can be concluded that macrocrack is expected to initiate at the material point with high damage value and its propagation would be along the direction of damage zone extension. The physical basis of this proposition is as follows: when a material element is loaded exter-

nally, part of the supplied energy is dissipated due to damage event, which is quantified through the damage variable, see Equation (3), and failure appears as a result of accumulated damage in the highly damaged process zone of the material.

The current approach provides a convenient and effective tool for examining stress states, failure modes, and damage propagation patterns and allows accurate monitoring of damage initiation and progression in unidirectional composites. Although the notch geometry considered is a circular hole, other types of geometrical discontinuities, such as macrocracks, elliptical holes etc. or multiple notches, can readily be analyzed with the aid of finite element technique. The proposed anisotropic damage model has been extended to characterize the damage response of crossed and angled laminates and found to be satisfactory [12,13].

REFERENCES

1. Reifsnider, K. L., (ed.). 1982. "Damage in Composite Materials: Basic Mechanisms, Accumulation, Tolerance and Characterization," *ASTM STP 775.*
2. Allix, O., P. Ladeveze, E. L. Dantec and E. Vittecoq. 1990. "Damage Mechanics for Composite Laminates under Complex Loading," in *Yielding, Damage, and Failure of Anisotropic Solids* J. P. Boehler (ed.), London: Mechanical Engineering Publications, EGF5, pp. 551–569.
3. Kamimura, K. 1985. "Continuum Damage Approach to Mechanical Behavior of Damaged Laminate and a Modelling of Damage Parameter," in *Mechanical Characterization of Load Bearing Fiber Composite Laminates,* A. H. Cardon and G. Verchery (ed.), Elsevier Applied Science Publishers Ltd., pp. 115–126.
4. Talreja, R. 1990. "Internal Variable Damage Mechanics of Composite Materials," in *Yielding, Damage, and Failure of Anisotropic Solids,* J. P. Boehler (ed.), London: Mechanical Engineering Publications, EGF5, pp. 509–533.
5. Allen, D. H. and J. W. Lee. 1990. "Matrix Cracking in Laminated Composites under Monotonic and Cyclic Loading," *ASME-AD,* 3:65–75.
6. Chow, C. L., F. Yang and A. Asundi. 1992. "A Method of Nonlinear Damage Analysis for Anisotropic Materials and Its Application to Thin Composite Laminates," *Int. J. of Damage Mechanics,* 1:347–366.
7. Chow, C. L. and F. Yang. 1994. "Inelastic Finite Element Analysis of Fiber Reinforced Composite Laminates with Damage," *Durability, and Damage Tolerance,* ASME AD, 34:111–136.
8. Schapery, R. A. 1990. "A Theory of Mechanical Behavior of Elastic Media with Growing Damage and Other Changes in Structure," *J. Mech. Phys. Solids,* 38:215–253.
9. Post, D. 1987. "Moiré Interferometry," in *Handbook of Experimental Mechanics,* A. S. Kobayashi (ed.), Englewood Cliffs: Prentice-Hall, Chapter 7.
10. Asundi, A. 1990. "Deformations in Glass-Fiber Woven Composite Using Moiré Interferometry," *Experimental Mechanics,* 30:230–233.
11. Asundi, A. and F. Yang. 1993. "Moiré Interferometry Strain Analysis Using FFT Technique for Fiber Reinforced Composite Laminates with Hole," in *Composite Properties and Applications, Proceedings of the 9th Int. Conf. on Composite Materials (ICBM/9),* A. Miravete (ed.), Madrid, pp. 874–881, July 12–16.
12. Chow, C. L. and F. Yang. 1994. "Elastic Damage Analysis of Interlaminar Stress Distributions in Symmetrical Composite Laminates with Edge Delamination Cracks," *Journal of Mechanical Engineering Science,* 208:1–11.
13. Chow, C. L. and F. Yang. 1997. "Three-Dimensional Inelastic Stress Analysis of Center Notched Composite Laminates with Damage," *International Journal of Damage Mechanics,* 6:23–50.